2024 IEEE 63rd Conference on Decision and Control (CDC)
December 16-19, 2024. MiCo, Milan, Italy

On The Controllability Preservation of Koopman Bilinear Surrogate Model

Joonwon Choi, Minhyun Cho, Hyunsang Park, Vishnu Vijay, and Inseok Hwang

Abstract— **In this paper, we analyze the controllability of the Koopman bilinear surrogate model of a controllable control affine system. The Koopman operator is a linear operator that can describe the evolution of an original (nonlinear) system by lifting the state using an observable. However, it has been proven that the lifted system may not necessarily be full-state controllable even if the original system is. Moreover, the infinite-dimensional nature of the Koopman operator means that a finite-dimensional approximation is often required in practice and thus, one cannot simply guarantee the lifted system to preserve the same controllability property of the original system. Motivated by this, we investigate how the controllability property of the original system affects that of the lifted system. We specifically focus on control affine systems, where one can construct a Koopman bilinear surrogate model using the infinitesimal generator of the Koopman operator. We assume there exists an admissible controller that can drive the state of the original control affine system to a desired state. Then, we present the controllability property of the corresponding Koopman bilinear surrogate model, constructed by the data-driven infinitesimal generator using generator extended dynamic mode decomposition (gEDMD). A numerical simulation example using a quadrotor model is presented to demonstrate the proposed results.**

I. INTRODUCTION

The Koopman operator is a linear but infinite-dimensional operator that can describe the evolution of the original (nonlinear) system state using an observable, the function defined on the state space [1]. The Koopman operator can provide benefits in analyzing the characteristics of complex systems by spectral analysis [2]; or can significantly alleviate the effort of designing a controller by describing the nonlinear dynamics in a linear framework [3]. As an extreme example, a nonlinear dynamics might be represented as a finite-dimensional linear time-invariant (LTI) system. Furthermore, the Koopman operator can be approximated using a data-driven method called extended dynamic mode decomposition (EDMD), without knowing the original system [1]. Thanks to these benefits, the Koopman operator has been widely utilized for various applications, such as fluid flow [4], [5] or estimation of human motion [6].

Along with active applications of the Koopman operator on the control and robotics applications, there have been several attempts to analyze the controllability property using the lifted system. For instance, the relationship between a Koopman bilinearization and a control affine system was investigated in [7] to check the controllability of the original system through the lifted system. In [8], the Koopman controllability gramian was introduced to check the controllability of the lifted system. The observability, the dual of the controllability, has been also investigated in [9].

On the other hand, there have been relatively few researches on the existence of a controllable lifted system when the original system is controllable. Many existing works simply assume the lifted system is controllable (or stabilizable) and design controllers accordingly. However, as shown in [2], the lifted system might not be completely controllable, i.e., full-state controllable, even if the original system is completely controllable. In [10], the authors proposed the infinite-dimensional extension of the Lie algebra rank condition (LARC) to verify the controllable submanifold of the lifted system, and showed the lifted system is unlikely to be completely controllable unless some restrictive conditions are satisfied.

In addition to the aforementioned findings, the Koopman operator might require approximations in practice due to its infinite-dimensional nature. To address this issue, the Koopman operator is often projected onto a finite-dimensional space using the Galerkin projection [1] and EDMD is known to converge to the result of the Galerkin projection with a sufficient amount of data [11]–[13]. Nevertheless, in real-world applications where one only has a finite amount of data, EDMD and its variations suffer from both projection error and finite-data error. Accordingly, one cannot always guarantee that the controllability property of the original system is preserved in the lifted system.

Motivated by this, we aim to investigate if the lifted system generated in a data-driven manner, such as EDMD or generator EDMD (gEDMD), is controllable if the original system is controllable. More specifically, given the knowledge that the original system is controllable in the domain of interest, we analyze if the lifted system can preserve such controllability. We specifically focus on the continuous-time control affine system and its Koopman bilinear surrogate model which describes the evolution of the observables using an infinitesimal generator [11], [12]. Then, we prove the corresponding Koopman bilinear surrogate model is output controllable, if there is no finite-data error, and output $\epsilon-$controllable in probability, if the infinitesimal generator is approximated from finite data.

Our contributions in this paper are as follows: 1) We analyze the controllability of the Koopman bilinear surrogate model generated from a control-affine system. Assuming

The authors would like to acknowledge that this work is supported by NSF CNS-1836952.

The authors are with the School of Aeronautics and Astronautics, Purdue University, West Lafayette, IN 47907 USA (e-mail: choi774@purdue.edu; cho515@purdue.edu; park1375@purdue.edu; vvijay@purdue.edu; ihwang@purdue.edu

there exists an admissible controller that drives the original system to a desired state, we show how the controllability property changes according to the conditions on the infinitesimal generators; and 2) we present numerical simulation results using a quadrotor model constructed by the infinitesimal generator to validate the proposed controllability properties.

The rest of the paper is organized as follows: In Section II, the preliminaries on the Koopman operator for control affine systems are presented. Section III provides a detailed analysis of the controllability property of the Koopman bilinear surrogate models. In Section IV, the numerical simulation results are presented and discussed. Lastly, the conclusion is given in Section V.

II. Preliminaries

To begin with, we consider a continuous-time autonomous system which is defined as:

$$\dot{\boldsymbol{x}}(t) = g_0(\boldsymbol{x}(t)) \tag{1}$$

where $\boldsymbol{x}(t) \in \mathbb{X}$ is the state at time t and $\mathbb{X} \subset \mathbb{R}^n$ is a compact set. Let observable $\varphi(\boldsymbol{x}(t))$ be a square-integrable function, i.e., $\varphi(\boldsymbol{x}(t)) \in L^2(\mathbb{X})$. Then, the Koopman semigroup or continuous time Koopman operator $\mathcal{K}^t$ satisfies the following equation [1]:

$$\mathcal{K}^t \varphi(\boldsymbol{x}(t_0)) = \varphi(\boldsymbol{x}(t)). \tag{2}$$

The corresponding infinitesimal generator of the Koopman operator, $\mathcal{L} : D(\mathcal{L}) \subset L^2(\mathbb{X}) \to L^2(\mathbb{X})$ is defined as

$$\mathcal{L} = \lim_{t \to 0} \frac{\mathcal{K}^t - I}{t} \tag{3}$$

where $D(\mathcal{L})$ is the domain of $\mathcal{L}$ and I is the identity matrix. As a result, one can represent the state evolution of the system (1) using the time-varying observable $\boldsymbol{z}(t) = \mathcal{K}^t \varphi(\boldsymbol{x}(t_0)) \in L^2(\mathbb{X})$ which is the solution of $\dot{\boldsymbol{z}}(t) = \mathcal{L}\boldsymbol{z}(t)$ [11].

However, equation (3) is difficult to be directly applied in practice because it is infinite-dimensional. To address this issue, one can project $\mathcal{L}$ onto a finite-dimensional space spanned by a finite number of bases. Let $\mathbb{V}$ be a finite-dimensional space spanned by bases $\psi_1(\boldsymbol{x}), \psi_2(\boldsymbol{x}), \cdots, \psi_N(\boldsymbol{x}) \in D(\mathcal{L})$,

$$\mathbb{V} := span\{\psi_i(\boldsymbol{x}), i = 1, \cdots, N\}, \tag{4}$$

where $\boldsymbol{x} = \boldsymbol{x}(t)$ and time t is omitted for brevity. Then, the Galerkin projection of $\mathcal{L}$ onto $\mathbb{V}$, $\mathcal{L}_{\mathbb{V}}$, can be computed as $\mathcal{L}_{\mathbb{V}}^T = AC^{-1}$. The (i, j) element of $C, A \in \mathbb{R}^{N \times N}$ is defined as [1], [14]

$$C_{ij} = \langle \psi_i(\boldsymbol{x}), \psi_j(\boldsymbol{x}) \rangle_\rho, \;\; A_{ij} = \langle \mathcal{L}\psi_i(\boldsymbol{x}), \psi_j(\boldsymbol{x}) \rangle_\rho \tag{5}$$

where $\langle \cdot, \cdot \rangle_\rho$ represents the inner product using a probability density ρ on $\mathbb{X}$, where one can draw samples with respect to ρ for the data-driven approach introduced later part of this section. In other words,

$$C_{ij} = \int_{\mathbb{X}} \psi_i(\boldsymbol{x})^* \psi_j(\boldsymbol{x}) \rho(\boldsymbol{x}) d\boldsymbol{x}, \tag{6}$$

$$A_{ij} = \int_{\mathbb{X}} \mathcal{L}\psi_i(\boldsymbol{x})^* \psi_j(\boldsymbol{x}) \rho(\boldsymbol{x}) d\boldsymbol{x}. \tag{7}$$

Accordingly, one can represent the propagation of the state using the finite-dimensional generator $\mathcal{L}_{\mathbb{V}}$ instead of $\mathcal{L}$.

However, the integration (6) and (7) are typically impossible to compute analytically [14]. Instead, one can use the generator extended dynamic mode decomposition (gEDMD) to approximate $\mathcal{L}_{\mathbb{V}}$ using the given data, i.e., a pure data-driven approach [11]–[13]. Let the m number of samples of the state, $\boldsymbol{x}_1, \boldsymbol{x}_2, \cdots, \boldsymbol{x}_m$, are given, thereby consisting the following matrices:

$$\Psi = [\psi(\boldsymbol{x}_1), \psi(\boldsymbol{x}_2), \cdots, \psi(\boldsymbol{x}_m)] \tag{8}$$

$$\mathcal{L}\Psi = [\mathcal{L}\psi(\boldsymbol{x}_1), \mathcal{L}\psi(\boldsymbol{x}_2), \cdots, \mathcal{L}\psi(\boldsymbol{x}_m)] \tag{9}$$

where $\psi(\boldsymbol{x}_i) = [\psi_1(\boldsymbol{x}_i), \psi_2(\boldsymbol{x}_i), \cdots, \psi_N(\boldsymbol{x}_i)]^T$ and $\mathcal{L}\psi(\boldsymbol{x}_i) = [\mathcal{L}\psi_1(\boldsymbol{x}_i), \mathcal{L}\psi_2(\boldsymbol{x}_i), \cdots, \mathcal{L}\psi_N(\boldsymbol{x}_i)]^T$. Then, the approximation of $\mathcal{L}_{\mathbb{V}}$ using m samples, $\tilde{\mathcal{L}}_m$, can be obtained as $\tilde{\mathcal{L}}_m = \tilde{A}_m \tilde{C}_m^{-1}$, where $\tilde{C}_m \in \mathbb{R}^{n \times n} = \Psi\Psi^T$ and $\tilde{A}_m \in \mathbb{R}^{n \times n} = (\mathcal{L}\Psi)\Psi^T$ [13].

The infinitesimal generator $\mathcal{L}$ can be extended to the Koopman bilinear surrogate model to handle a control-affine system. Let the dynamics of the control affine system be given as

$$\dot{\boldsymbol{x}}(t) = g_0(\boldsymbol{x}(t)) + \sum_{i=1}^{n_c} g_i(\boldsymbol{x}(t)) u_i(t), \tag{10}$$

where $u_i(t)$ is the $i-$th component of the control input $\boldsymbol{u}(t) = [u_1(t), u_2(t), \cdots, u_{n_c}(t)]^T \in \mathbb{U} \subset \mathbb{R}^{n_c}$ and $\mathbb{U}$ is bounded. $g_1, \cdots, g_{n_c} : \mathbb{R}^n \to \mathbb{R}^n$ are non-drift terms. Furthermore, we assume (10) is controllable, i.e., for a given initial state at time t_0, $\boldsymbol{x}(t_0)$, and desired state at t_f, $\boldsymbol{x}_d(t_f)$, there exists an admissible controller $\boldsymbol{u}(t)$ that drives $\boldsymbol{x}(t_0)$ to $\boldsymbol{x}_d(t_f)$. It is worth noting that we do not specify a particular type of nonlinear system controllability, such as the small-time local controllability. The objective of this paper is to investigate the existence of a controller that can drive the lifted system to a desired lifted state, aided by the existence of $\boldsymbol{u}(t)$ for the original system.

The corresponding Koopman bilinear surrogate model can be described using a set of infinitesimal generators as

$$\dot{\boldsymbol{z}}(t) = \mathcal{L}^u(t)\boldsymbol{z}(t) = \mathcal{L}^{e_0}\boldsymbol{z}(t) + \sum_{i=1}^{n_c} (\mathcal{L}^{e_i} - \mathcal{L}^{e_0})\boldsymbol{z}(t) u_i(t), \tag{11}$$

by setting $\mathcal{L}^u(t) = \mathcal{L}^{e_0} + \sum_{i=1}^{n_c} (\mathcal{L}^{e_i} - \mathcal{L}^{e_0}) u_i(t)$, where $\mathcal{L}^{e_i}$ represents the infinitesimal generator for the autonomous system corresponding to a constant input $u_i(t) = e_i$, the $i-$th basis of $\mathbb{R}^{n_c}$. In other words, (11) can be obtained as a combination of $n_c + 1$ autonomous systems, where each of them corresponds to a constant input $e_i, \; \forall i = 0, 1, \cdots, n_c$, assuming $e_0 = 0$. The corresponding projected generator $\mathcal{L}_{\mathbb{V}}^u(t)$ and approximated generator $\tilde{\mathcal{L}}_m^u(t)$ can be obtained using the same method in (5)-(9) [11], [12].

In the following section, we investigate how the controllability of the original control affine system (10) is affected by the Koopman bilinear surrogate model corresponding to each generator, $\mathcal{L}^u$, $\mathcal{L}_{\mathbb{V}}^u$, and $\tilde{\mathcal{L}}_m^u$, respectively.

III. Controllability preservation of Koopman bilinear surrogate model

For the sake of simplicity, we assume the state $\boldsymbol{x}$ can be expressed using the dictionary $\psi(\boldsymbol{x})$; and the same for the observable $\varphi(\boldsymbol{x})$.

Assumption 1: The state $\boldsymbol{x}$ can be represented using the dictionary $\psi(\boldsymbol{x})$ or observable $\varphi(\boldsymbol{x})$, i.e., there exist $h_{(\cdot)}$ and H_N such that $\boldsymbol{x} = H_N\psi(\boldsymbol{x}) = \sum_{i=1}^{\infty} h_i\varphi_i(\boldsymbol{x})$.

Note that Assumption 1 has been widely applied in various applications using the Koopman operator, particularly in the robotics field. For instance, Assumption 1 automatically holds if the full-state dictionary is available [15], [16].

A. Infinite dimensional generator $\mathcal{L}^u$

In this subsection, we investigate the controllability of the Koopman bilinear surrogate model (11), where the Koopman generator is given as the infinite-dimensional generator $\mathcal{L}^u(t)$. Although we assume the original system (10) can drive an initial state to a desired state $\boldsymbol{x}_d(t_f)$, it does not guarantee the bilinear surrogate model (11) is also completely controllable. Nevertheless, from Assumption 1, $\boldsymbol{x}(t) = \sum_{i=1}^{\infty} h_i\varphi(\boldsymbol{x}(t))$ and thus, one can at least guarantee (11) delivers the subset of the observable that corresponds to the state.

Proposition 1: If Assumption 1 holds, there exists an output controllable infinite-dimensional Koopman bilinear surrogate model (11) corresponding to the control affine system (10).

Proof Let the initial state $\boldsymbol{x}(t_0)$ and desired state $\boldsymbol{x}_d(t_f)$ are given. Since there exists an admissible controller $\boldsymbol{u}(t)$ that drives the system (10) from $\boldsymbol{x}(t_0)$ to $\boldsymbol{x}_d(t_f)$; and there exists $h_{(\cdot)}$ $s.t.$ $\sum_{i=1}^{\infty} h_i\varphi(\boldsymbol{x}(t)) = \boldsymbol{x}(t)$ from Assumption 1, based on $\boldsymbol{x}_d(t_f) = \sum_{i=1}^{\infty} h_i\varphi(\boldsymbol{x}(t_f))$ and $\boldsymbol{x}(t_0) = \sum_{i=1}^{\infty} h_i\varphi(\boldsymbol{x}(t_0))$, $\boldsymbol{u}(t)$ also drives the subset of the observable corresponding to the state as desired. Accordingly, since there exists an admissible controller $\boldsymbol{u}(t)$ for given $\boldsymbol{x}(t_0)$ and $\boldsymbol{x}_d(t_f)$, the Koopman bilinear surrogate model (11) is output controllable. ■

Proposition 1 aligns with the findings in [2] that the lifted system does not always guarantee the complete global controllability, even if the original system is globally controllable. It also agrees with [10], where the authors rigorously extend the Lie algebra rank condition (LARC) to an infinite-dimensional system to specify the controllable submanifold of the Koopman bilinear surrogate model (11).

B. Projected generator $\mathcal{L}^u_{\mathbb{V}}$

Although the Koopman bilinear surrogate model (11) preserves its controllability on the state $\boldsymbol{x}$, one might need to project $\mathcal{L}^u(t)$ onto a finite-dimensional space to be useful for real-world applications. The projected Koopman bilinear surrogate model using the projected Koopman generator $\mathcal{L}^u_{\mathbb{V}}(t)$ can be defined as follows [11]:

$$\begin{aligned}\dot{\boldsymbol{z}}_{\mathbb{V}}(t) =& \mathcal{L}^u_{\mathbb{V}}(t)\boldsymbol{z}_{\mathbb{V}}(t)\\ =& \mathcal{L}^{e_0}_{\mathbb{V}}\boldsymbol{z}_{\mathbb{V}}(t) + \sum_{i=1}^{n_c}(\mathcal{L}^{e_i}_{\mathbb{V}} - \mathcal{L}^{e_0}_{\mathbb{V}})\boldsymbol{z}_{\mathbb{V}}(t)u_i(t) \qquad (12)\end{aligned}$$

where $\boldsymbol{z}_{\mathbb{V}}(t_0) = P_{\mathbb{V}}\varphi(\boldsymbol{x}(t_0))$ and $P_{\mathbb{V}}$ is the projection onto $\mathbb{V}$.

The projected generator $\mathcal{L}^u_{\mathbb{V}}(t)$ suffers from projection errors depending on the choice of the dictionary $\psi(\boldsymbol{x})$ [11], [12], [17] and thus, might not preserve the exact propagation of the state in Proposition 1. Nevertheless, if $\psi(\boldsymbol{x})$ spans the invariant space of $\mathcal{L}^{e_i}_{\mathbb{V}}$, $\forall i = 0, 1, \cdots, n_c$, the projected model (12) can describe the propagation of the dictionary in $\mathbb{V}$ using the finite-dimensional $\psi(\boldsymbol{x})$ [18].

Assumption 2: The dictionary forms an invariant space of infinitesimal generators $\mathcal{L}^{e_i}_{\mathbb{V}}$ $\forall i = 0, 1, \cdots, n_c$, i.e., $span\{\psi_1, \psi_2, \cdots, \psi_N\}$ is invariant under $\mathcal{L}^u_{\mathbb{V}}(t)$.

Accordingly, from Assumption 2, one can expect that the Koopman bilinear surrogate model (12) preserves the exact propagation of $\psi(\boldsymbol{x})$ without the projection error.

Corollary 1: If Assumptions 1 and 2 hold, there exists an output controllable Koopman bilinear surrogate model (12) corresponding to the control affine system (10).

Proof The proof is identical to that of Proposition 1 and thus omitted here. ■

Remark 1: If Assumption 2 does not hold, the projection error can be alleviated by properly increasing the size of the dictionary N. For instance, the conditions that make $\mathcal{L}^{e_i}_{\mathbb{V}}$ converge to $\mathcal{L}^{e_i}$ as $N \to \infty$ was presented in [13], while the error between the infinite-dimensional generator and projected generator was explicitly introduced in [17]. Accordingly, although the exact output controllability might be lost, the projection error can be gradually eliminated by increasing N. The rigorous analysis on the Koopman bilinear surrogate model with the projection error will remain as future work.

In the following section, we investigate the controllability property of the Koopman bilinear surrogate model using the generator extended dynamic mode decomposition (gEDMD) and corresponding infinitesimal generator $\tilde{\mathcal{L}}^u_m$.

C. Finite-data approximated generator $\tilde{\mathcal{L}}^u_m$

The gEDMD (8)-(9) is a variation of the standard EDMD that can approximate the infinitesimal generator in a data-driven manner. The Koopman bilinear surrogate model using the gEDMD can be represented as [11]

$$\begin{aligned}\dot{\tilde{\boldsymbol{z}}}_m(t) =& \tilde{\mathcal{L}}^u_m(t)\tilde{\boldsymbol{z}}_m(t)\\ =& \tilde{\mathcal{L}}^0_m\tilde{\boldsymbol{z}}_m(t) + \sum_{i=1}^{n_c}(\tilde{\mathcal{L}}^{e_i}_m - \tilde{\mathcal{L}}^0_m)\tilde{\boldsymbol{z}}_m(t)u_i(t), \qquad (13)\end{aligned}$$

where $\tilde{\boldsymbol{z}}_m(t_0) = P_{\mathbb{V}}\varphi(\boldsymbol{x}(t_0))$.

In [11], [12], it has been proven that the infinitesimal generator computed by gEDMD, $\tilde{\mathcal{L}}^u_m(t)$, converges to the $\mathcal{L}^u_{\mathbb{V}}(t)$ if the number of the samples m is sufficiently large and the samples are collected following the probability density ρ from $\mathbb{X}$.

Assumption 3: The independent and identically distributed (i.i.d.) samples $\boldsymbol{x}_1, \boldsymbol{x}_2, \cdots, \boldsymbol{x}_m$ are drwan from $\mathbb{X}$ with respect to ρ.

Nevertheless, the convergence of gEDMD is an asymptotic property as $m \to \infty$ and thus, $\tilde{\mathcal{L}}^u_m(t)$ still suffers from

the finite data error in practice. Accordingly, the Koopman bilinear surrogate model (13) might not preserve the exact propagation of observable even though Assumption 2 holds.

To address the controllability of the approximated Koopman bilinear surrogate model (13), we first introduce the term $\epsilon-$*controllable in probability*. The system is $\epsilon-$controllable in probability $1-\delta$ at $\boldsymbol{x}(t_0)$ if there exists an admissible controller $\boldsymbol{u}(t)$ that drives the initial state toward the desired state $\boldsymbol{x}_d(t_f)$ satisfying $P(\|\boldsymbol{x}_d(t_f)-\boldsymbol{x}(t_f)\|^2 \leq \epsilon) \geq 1-\delta$, where $\delta \in (0,1)$ [19]–[21]. In (13), we further focus on the subset of $\tilde{\boldsymbol{z}}_m$, defining the output $\epsilon-$controllable in probability as follows:

***Definition** 1:* (*Output $\epsilon-$controllable in probability*) The system is output $\epsilon-$controllable in probability $1-\delta$ at $\boldsymbol{x}(t_0)$ if there exists an admissible controller $\boldsymbol{u}(t)$ such that steering the output $\boldsymbol{y}(t)$ to a desired output $\boldsymbol{y}_d(t_f)$ satisfying $P(\|\boldsymbol{y}_d(t_f)-\boldsymbol{y}(t_f)\|^2 \leq \epsilon) \geq 1-\delta$.

***Proposition** 2:* If Assumptions 1-3 hold, for arbitrary $\delta \in (0,1)$ and $\epsilon > 0$, the Koopman bilinear surrogate model (13) corresponding to the control affine system (10) is output $\epsilon-$controllable in probability $1-\delta$ if m is sufficiently large.

Proof From [11], [12], for arbitrary δ and $\bar{\epsilon}$, given $\boldsymbol{z}_{\mathbb{V}}(t_0) = \tilde{\boldsymbol{z}}_m(t_0)$, there exists the minimum number of samples $\underline{m} < \infty$ such that the following inequality holds:

$$P(\|\boldsymbol{z}_{\mathbb{V}}(t)-\tilde{\boldsymbol{z}}_m(t)\| \leq \bar{\epsilon}) > 1-\delta, \tag{14}$$

if $m \geq \underline{m} = \mathcal{O}(\frac{N}{\bar{\epsilon}^2\delta})$, where $\|\cdot\|$ is 2-norm; and $\boldsymbol{z}_{\mathbb{V}}(t)$ and $\tilde{\boldsymbol{z}}_m(t)$ are propagated according to (12) and (13), respectively, but using the same controller $\boldsymbol{u}(t)$. For the details on computing $\underline{m}$ can be found in [11], [12]. Meanwhile, the error between the true state and the prediction from (13) satisfies the following inequality:

$$\begin{aligned}&\|\boldsymbol{x}(t)-H_N\tilde{\boldsymbol{z}}_m(t)\| \\ &\quad\leq \|\boldsymbol{x}(t)-H_N\boldsymbol{z}_{\mathbb{V}}(t)\| + \|H_N\boldsymbol{z}_{\mathbb{V}}(t)-H_N\tilde{\boldsymbol{z}}_m(t)\|\end{aligned} \tag{15}$$

Since $\|\boldsymbol{x}(t)-H_N\boldsymbol{z}_{\mathbb{V}}(t)\| = 0$ from Assumption 2, i.e., the projection error term diminishes,

$$\begin{aligned}\|\boldsymbol{x}(t)-H_N\tilde{z}_m(t)\| &\leq \|H_N\boldsymbol{z}_{\mathbb{V}}(t)-H_N\tilde{\boldsymbol{z}}_m(t)\| \\ &\leq \|H_N\|\|\boldsymbol{z}_{\mathbb{V}}(t)-\tilde{\boldsymbol{z}}_m(t)\|.\end{aligned} \tag{16}$$

Thus, by setting $\sqrt{\epsilon} = \|H_N\|\bar{\epsilon}$,

$$\begin{aligned}&P(\|\boldsymbol{x}(t)-H_N\tilde{z}_m(t)\|^2 \leq \epsilon) \\ &= P(\|\boldsymbol{x}(t)-H_N\tilde{z}_m(t)\| \leq \sqrt{\epsilon}) \\ &\geq P(\|H_N\|\|\boldsymbol{z}_{\mathbb{V}}(t)-\tilde{\boldsymbol{z}}_m(t)\| \leq \sqrt{\epsilon}) \\ &= P(\|\boldsymbol{z}_{\mathbb{V}}(t)-\tilde{\boldsymbol{z}}_m(t)\| \leq \bar{\epsilon}) \geq 1-\delta.\end{aligned} \tag{17}$$

Accordingly, there exists a finite $m \geq \underline{m}$ such that $\|\boldsymbol{x}(t_f)-H_N\tilde{\boldsymbol{z}}_m(t_f)\|^2 \leq \epsilon$ with probability $1-\delta$ for any given $\epsilon > 0$ and δ. ■

***Corollary** 2:* If Assumption 2 does not hold but the projection error can be bounded by $\bar{e}_r \in \mathbb{R} > 0$, i.e., $0 < \|\boldsymbol{x}(t)-H_N\boldsymbol{z}_{\mathbb{V}}(t)\| \leq \bar{e}_r$, for arbitrary $\delta \in (0,1)$ and $\epsilon > \bar{e}_r^2$, the Koopman bilinear surrogate model (13) is output $\epsilon-$controllable in probability $1-\delta$ if m is sufficiently large.

Proof In (15), since $0 < \|\boldsymbol{x}(t)-H_N\boldsymbol{z}_{\mathbb{V}}(t)\| \leq \bar{e}_r$, by setting $\sqrt{\epsilon} = \|H_N\|\bar{\epsilon}+\bar{e}_r$,

$$\begin{aligned}&P(\|\boldsymbol{x}(t)-H_N\tilde{z}_m(t)\|^2 \leq \epsilon) \\ &= P(\|\boldsymbol{x}(t)-H_N\tilde{z}_m(t)\| \leq \sqrt{\epsilon}) \\ &\geq P(\|H_N\|\|\boldsymbol{z}_{\mathbb{V}}(t)-\tilde{\boldsymbol{z}}_m(t)\| \leq \sqrt{\epsilon}-\bar{e}_r) \\ &= P(\|\boldsymbol{z}_{\mathbb{V}}(t)-\tilde{\boldsymbol{z}}_m(t)\| \leq \bar{\epsilon}) \geq 1-\delta.\end{aligned} \tag{18}$$

Accordingly, same as Proposition 2, there exists $m \geq \underline{m}$ such that $\|\boldsymbol{x}(t_f)-H_N\tilde{\boldsymbol{z}}_m(t_f)\|^2 \leq \epsilon$ with probability $1-\delta$. ■

In summary, the Koopman bilinear surrogate model obtained from a controllable control affine system becomes $\epsilon-$controllable in probability and thus, the Koopman bilinear surrogate model using the gEDMD (13) is not exactly output controllable but moves toward the given desired state arbitrarily closely if Assumption 2 holds; and up to a certain closeness proportional to $\bar{e}_r^2$ if there exists the projection error.

IV. Numerical simulation

A. $SO(2)$ *qaudrotor model*

We provide numerical simulation results using a planar 3DOF quadrotor model. The nonlinear dynamics of the quadrotor can be written as

$$\begin{aligned}\dot{\mathbf{p}} &= v, \\ \dot{\mathbf{v}} &= -ge_2 + (1/m_s)R^T\Sigma_{i=1}^2 T_i e_2 \\ \dot{\theta} &= \omega, \\ \dot{\omega} &= (l/J_y)\Sigma_{i=1}^2(-1)^i T_p,\end{aligned} \tag{19}$$

where $R \in \mathbb{R}^2$ is the rotation matrix in SO(2) with angle θ, $\mathbf{p}$ is the position, $\mathbf{v}$ is the velocity, ω is the angular velocity, J_y is the rotational inertia, m_s is the mass of the quadrotor, l is the arm length from the center of gravity to the rotors, g is the gravitational acceleration, T_i is the thrust from each rotor i, and $e_2 = [0,1]^T$ is the unit vector in $z-$direction of the global frame. The parameters of the quadrotor model are borrowed from Holybro X500[1] with some minor modifications.

We substitute $T_i = \frac{1}{2}mg + \Delta T_i$, where ΔT_i denotes the thrust deviation from the trim thrust $\frac{1}{2}mg$ for $i = 1,2$. The dictionary up to $k-$th order is defined as $\psi(\boldsymbol{x}) = [\bar{\psi}_1(\boldsymbol{x}), \bar{\psi}_2(\boldsymbol{x})]^T$ where

$$\begin{aligned}\bar{\psi}_1(\boldsymbol{x}) &= \left[\mathbf{p}^T,\, \mathbf{v}^T,\, \theta,\, \omega,\, 1\right], \\ \bar{\psi}_2(\boldsymbol{x}) &= \left[\sin\theta,\, \cos\theta,\, \cdots,\, \omega^k\sin\theta,\, \omega^k\cos\theta\right].\end{aligned} \tag{20}$$

Then, from the recursive relation of the observables in $\bar{\psi}_2(\mathbf{x})$

$$\begin{aligned}\mathcal{L}\psi_{2,2j+1} &= \psi_{2,2j+4} + (jl/J_y)\,\psi_{2,2j-1}\Sigma(-1)^i\Delta T_i, \\ \mathcal{L}\psi_{2,2j+2} &= -\psi_{2,2j+3} + (jl/J_y)\,\psi_{2,2j}\Sigma(-1)^i\Delta T_i,\end{aligned} \tag{21}$$

for $\forall j < k$, where $\psi_{q,p}$ means the p-th element in $\bar{\psi}_q$.

Facilitating the results in [22], where the three-dimensional quadrotor analysis was conducted, one can verify that the lifted function space of the planar quadrotor dynamics (19)

[1]https://github.com/PX4/PX4-gazebo-models

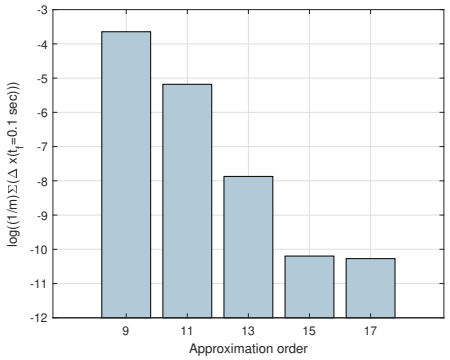

Fig. 1: Semi-log plot of the mean projection error computed from 100 trajectories with each distinct dictionary size $N = 9, 11, 13, 15, 17$

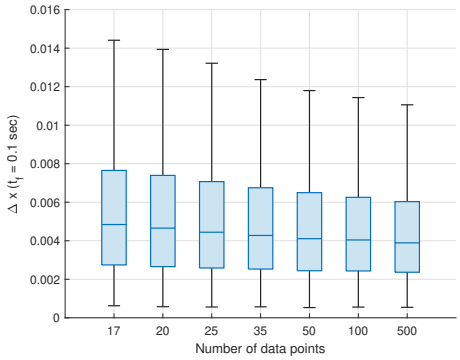

Fig. 3: Box plot of the sampled relative error between the true system state $\boldsymbol{x}(t)$ and the state of approximated Koopman bilinear surrogate model using $\tilde{\mathcal{L}}^u_m$, $H_N\tilde{\boldsymbol{z}}_m(t)$.

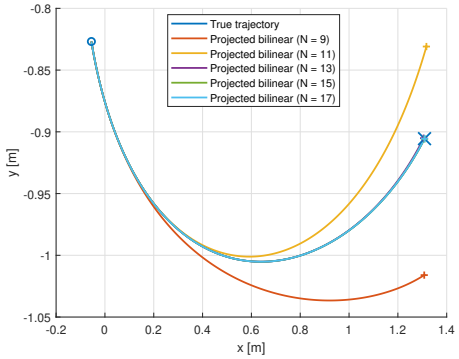

Fig. 2: Trajectories generated by the projected infinitesimal generator $\mathcal{L}^u_{\mathbb{V}}$

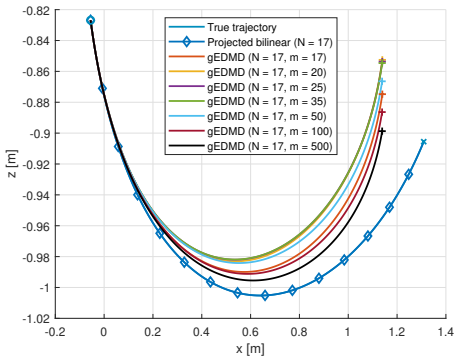

Fig. 4: Trajectories generated by the approximated infinitesimal generator $\tilde{\mathcal{L}}^u_m$

can be spanned by the countably infinite size of dictionary $\psi(\boldsymbol{x})$, i.e., if $k \to \infty$. In other words, one can exactly represent the dynamics of the quadrotor using $\psi(\boldsymbol{x})$ as $N \to \infty$; and the projection error converges to 0 accordingly. Based on this, we first generate the projected Koopman bilinear surrogate models (12) by increasing k from 1 to 5, where $N = 2k + 7$. Then, the relative error is computed as

$$\Delta\boldsymbol{x}(t) = \frac{||\boldsymbol{x}(t) - H_N\boldsymbol{z}_{\mathbb{V}}(t)||_2}{||\boldsymbol{x}(t)||_2} \tag{22}$$

which shows the accuracy of the projected Koopman bilinear surrogate model with respect to the true system. The log mean error is obtained by computing the mean of the relative error, $\log((1/m_I)\Sigma_{i=1}^{m_I}\Delta\mathbf{x}_i(t_f))$, from 100 randomly generated trajectories, i.e., $m_I = 100$, where $\Delta\mathbf{x}_i(t_f)$ is computed at the $i-$th simulation. The initial states of random trajectories are sampled from a polytope $\mathcal{P} = \{\mathbf{x} \in \mathbb{R}^6 | \ \mathbf{p} \in [-1.5, 1.5]^2, \ \mathbf{v} \in [-1.0, 1.0]^2, \ \theta \in [-\pi/9, \pi/9], \ \omega \in [-\pi/18, \pi/18]\}$ following the uniform distribution. The trajectories are generated under the same control input $\mathbf{u} = K\boldsymbol{x}(t)$ where the cascade controller and its gain K are designed by following [23].

Figure 1 shows the relative approximation error of the projected Koopman bilinear model as N increases. The final time for the projection error computation is set as $t_f = 0.1$ seconds. As one can easily observe, the error exponentially reduces as N increases which agrees with our expectation that the projection error will be reduced as the size of $\psi(\boldsymbol{x})$ is increased. Meanwhile, Figure 2 describes the predicted trajectories generated for 1.5 seconds. In the figure, the circle represents the shared initial position, the blue line is the true trajectory, and the other colored lines represent the trajectory using the different Koopman bilinear surrogate models corresponding to distinct $N = 9$, 11, 13, 15, and 17, respectively. It is noticeable that the trajectory generated from the Koopman bilinear surrogate model almost coincides with the true trajectory if N is sufficiently large, i.e., $N = 17$, thereby proving the projection error diminishes as $k \to \infty$.

B. Simulation results using gEDMD and Approximated Koopman bilinear surrogate model

We constructed the approximated infinitesimal generator $\tilde{\mathcal{L}}^u_m$ using the samples generated from (19), but without knowing the model. In other words, we computed the approximated Koopman bilinear surrogate model in a purely data-driven manner using the gEDMD. To this end, we collected uniformly distributed samples from the same polytope $\mathcal{P}$ as the previous analysis. Note that the samples are collected

for each autonomous system, respectively. In other words, the samples are collected from three autonomous systems corresponding to $(\Delta T_1, \Delta T_2) \in \{(0,0),(1,0),(0,1)\}$, and then the infinitesimal generators $\tilde{\mathcal{L}}_m^{e0}$, $\tilde{\mathcal{L}}_m^{e1}$, and $\tilde{\mathcal{L}}_m^{e2}$ are computed, respectively. The value of k is set to be 17 in this simulation.

Figure 3 is the results of the Monte Carlo simulation showing the relative error between the true system and the approximated Koopman bilinear surrogate model obtained from the distinct number of samples, m, at $t_f = 0.1$. The relative error computation follows (22), but substituting $H_N \tilde{\boldsymbol{z}}_m(t)$ instead of $H_N \boldsymbol{z}_{\mathbb{V}}(t)$. We performed 100 Monte Carlo simulations per each m to compute the statistics. In the figure, the box represents 0.25 to 0.75 quantiles of the data, while the middle line is the median. It is clear that the relative error and its variance tend to decrease as m increases. However, there exists the non-zero error, i.e., $\Delta \boldsymbol{x} \neq 0$, due to the both projection and finite-data error. This also aligns with Proposition 2 and Corollary 2 where arbitrary error bound ϵ and confidence $1-\delta$ can be obtained if the number of samples m is sufficient.

Such a tendency is more clearly observed in Fig. 4 which presents the 1.5 seconds trajectory prediction results using gEDMD with different numbers of samples. In the figure, the circle represents the initial position of the quadrotor and the blue trajectory represents the true trajectory. Meanwhile, the other colored trajectories describe the trajectories generated from different $\tilde{\mathcal{L}}_m^u$ for each distinct number of samples, m. As one can easily notice, the trajectory tends to get closer to the true trajectory as m increases, as shown in Fig. 3. These results prove that one can represent the behavior of the system only using the given data, even if the original system is unknown. Furthermore, the generated Koopman bilinear surrogate model gradually retrieves the controllability property of the original system as the number of data increases according to Proposition 2 and Corollary 2. Thus, one can justify the existence of the controllable lifted system, given the knowledge that the original control affine system is controllable, if a sufficient amount of data is provided.

V. CONCLUSION

In this paper, we investigated the controllability property of the Koopman bilinear surrogate model, which is constructed from the data sampled from a controllable continuous-time control affine system. Assuming the dictionary can describe the state of the system, we analyzed that the Koopman bilinear surrogate models using the exact and projected infinitesimal generator become output controllable, and that of the approximated generator using the generator extended dynamic mode decomposition (gEDMD) becomes output $\epsilon-$controllable in probability, respectively. As future works, a more rigorous analysis on the effect of the projection error will be performed.

REFERENCES

[1] M. O. Williams, I. G. Kevrekidis, and C. W. Rowley, "A data–driven approximation of the Koopman operator: Extending dynamic mode decomposition," *Journal of Nonlinear Science*, vol. 25, pp. 1307–1346, 2015.

[2] D. Goswami and D. A. Paley, "Bilinearization, reachability, and optimal control of control-affine nonlinear systems: A Koopman spectral approach," *IEEE Transactions on Automatic Control*, vol. 67, no. 6, pp. 2715–2728, 2021.

[3] S. L. Brunton, M. Budišić, E. Kaiser, and J. N. Kutz, "Modern Koopman theory for dynamical systems," *arXiv preprint arXiv:2102.12086*, 2021.

[4] I. Mezić, "Analysis of fluid flows via spectral properties of the Koopman operator," *Annual review of fluid mechanics*, vol. 45, pp. 357–378, 2013.

[5] ——, "Spectral properties of dynamical systems, model reduction and decompositions," *Nonlinear Dynamics*, vol. 41, pp. 309–325, 2005.

[6] N. Powell, B. Liu, and A. J. Kurdila, "Koopman methods for estimation of motion over unknown, regularly embedded submanifolds," in *2022 American Control Conference (ACC)*. IEEE, 2022, pp. 2584–2591.

[7] S. Sinha, S. P. Nandanoori, T. Ramachandran, C. Bakker, and A. Singhal, "Data-driven resilience characterization of control dynamical systems," in *2022 American Control Conference (ACC)*. IEEE, 2022, pp. 2186–2193.

[8] E. Yeung, Z. Liu, and N. O. Hodas, "A Koopman operator approach for computing and balancing gramians for discrete time nonlinear systems," in *2018 Annual American Control Conference (ACC)*. IEEE, 2018, pp. 337–344.

[9] A. Mesbahi, J. Bu, and M. Mesbahi, "Nonlinear observability via Koopman analysis: Characterizing the role of symmetry," *Automatica*, vol. 124, p. 109353, 2021.

[10] W. Zhang and J.-S. Li, "Koopman bilinearization of nonlinear control systems," *arXiv preprint arXiv:2211.07112*, 2022.

[11] M. Schaller, K. Worthmann, F. Philipp, S. Peitz, and F. Nüske, "Towards reliable data-based optimal and predictive control using extended dmd," *IFAC-PapersOnLine*, vol. 56, no. 1, pp. 169–174, 2023.

[12] F. Nüske, S. Peitz, F. Philipp, M. Schaller, and K. Worthmann, "Finite-data error bounds for Koopman-based prediction and control," *Journal of Nonlinear Science*, vol. 33, no. 1, p. 14, 2023.

[13] J. J. Bramburger and G. Fantuzzi, "Auxiliary functions as Koopman observables: Data-driven analysis of dynamical systems via polynomial optimization," *Journal of Nonlinear Science*, vol. 34, no. 1, p. 8, 2024.

[14] S. Klus, F. Nüske, S. Peitz, J.-H. Niemann, C. Clementi, and C. Schütte, "Data-driven approximation of the Koopman generator: Model reduction, system identification, and control," *Physica D: Nonlinear Phenomena*, vol. 406, p. 132416, 2020.

[15] D. Bruder, X. Fu, R. B. Gillespie, C. D. Remy, and R. Vasudevan, "Data-driven control of soft robots using Koopman operator theory," *IEEE Transactions on Robotics*, vol. 37, no. 3, pp. 948–961, 2020.

[16] A. Jin, F. Zhang, and P. Huang, "Data-driven optimal control of tethered space robot deployment with learning based Koopman operator," *arXiv preprint arXiv:2307.07713*, 2023.

[17] C. Zhang and E. Zuazua, "A quantitative analysis of Koopman operator methods for system identification and predictions," *Comptes Rendus. Mécanique*, vol. 351, no. S1, pp. 1–31, 2023.

[18] L. C. Iacob, R. Tóth, and M. Schoukens, "Koopman form of nonlinear systems with inputs," *Automatica*, vol. 162, p. 111525, 2024.

[19] J. Klamka and L. Socha, "Some remarks about stochastic controllability," *IEEE Transactions on Automatic Control*, vol. 22, no. 5, pp. 880–881, 1977.

[20] A. Czornik and A. Swierniak, "On controllability with respect to the expectation of discrete time jump linear systems," *Journal of the Franklin Institute*, vol. 338, no. 4, pp. 443–453, 2001.

[21] M. Mariton, "On controlability of linear systems with stochastic jump parameters," *IEEE transactions on Automatic Control*, vol. 31, no. 7, pp. 680–683, 1986.

[22] V. Zinage and E. Bakolas, "Koopman operator based modeling for quadrotor control on SE(3)," *IEEE Control Systems Letters*, vol. 6, pp. 752–757, 2021.

[23] D. Mellinger, N. Michael, and V. Kumar, "Trajectory generation and control for precise aggressive maneuvers with quadrotors," *The International Journal of Robotics Research*, vol. 31, no. 5, pp. 664–674, 2012.